ALN-BASED PIEZOELECTRIC RESONATOR FOR INFRARED SENSING APPLICATION

Wan C. Ang[1,2], Piotr Kropelnicki[1], Humberto Campanella[1], Yao Zhu[1,2], Andrew B. Randles[1], Hong Cai[1], Yuandong A. Gu[1], Kam C. Leong[3], and Chuan S. Tan[2]

[1]Institute of Microelectronics, Agency of Science, Technology and Research (A*STAR), SINGAPORE

[2]Nanyang Technological University, SINGAPORE

[3]GLOBALFOUNDRIES Singapore Pte Ltd, SINGAPORE

ABSTRACT

This paper reports a highly sensitive aluminum nitride (AlN) based resonant uncooled infrared (IR) detector utilizing photo-sensitive and piezoelectric properties of polycrystalline AlN. The design, fabrication, and IR sensing characterization of the device are presented. Instead of resonant frequency shift, S_{21} magnitude shift was observed upon IR illumination under both vacuum and ambient measurements. Thus, photoresponse mechanism was proposed rather than thermal effect. An AlN resonator operating at 2.336 GHz with a quality factor (Q) of 830 exhibits an IR responsivity and detectivity of 166 kdB/W and 1.41×10^7 cm√Hz/W, respectively.

INTRODUCTION

With the discovery of exciting applications using miniaturized and portable IR detectors, micro-electro-mechanical-system (MEMS) based uncooled IR detectors are gaining increasing attention. As cooling system is not necessary, uncooled IR detectors have low weight, low power consumption, high reliability, low manufacturing and operation cost. With the broadband sensitivity, uncooled IR detectors are of particular interest in spectrometer applications. However, uncooled IR detectors have an overall lower performance and slower response compared with photon detectors.

Semiconductor-based resistive microbolometers are the most commercially successful uncooled IR detectors because they are relatively easy to fabricate compared with pyroelectric detectors [1] and have a better responsivity than thermoelectric detectors [2]. Since early 1990s, their performance has been improved with the advances in silicon micromachining technologies. However, they are tardily facing bottleneck in further enhancing their performance recently due to the inevasible high flicker (1/*f*) and Johnson noise. Hence, there is a necessity for novel technologies that could beat the sensing performance of photon detectors in addition to retain the advantages of uncooled detectors.

Resonant uncooled IR detector is the next promising candidate for IR detection due to the highest accuracy frequency readout. Furthermore, it draws much less power than a resistive microbolometer because no DC current is flowing through the sensing materials. Self-heating of a resonator can be easily controlled by minimizing the RF power level [3]. The device 1/*f* noise can be ignored owing to high frequency operation (from 100 MHz – 2.5 GHz). In 1985, IR sensing of quartz bulk acoustic wave (BAW) resonators was first reported [4], followed by a detailed analysis in thermal imaging application in year 1994 [5]. With the advances in MEMS technologies, quartz film bulk acoustic resonator (FBAR) has been reported to exhibit a noise-equivalent-temperature-difference (NETD) of less than 5 mK in year 2011 [6]. Because of the non-scalability and non-CMOS compatibility, quartz BAW resonators are facing difficulty in mass production. Different piezoelectric materials have been investigated to replace quartz including GaN [7], ZnO [8], and AlN [9]. Promising IR sensing characteristic of these materials has been demonstrated.

In this work, AlN-based piezoelectric resonator was designed, fabricated and characterized. Post-CMOS integration is feasible because AlN piezoelectric thin films with high quality and uniformity can be deposited by sputtering process on silicon substrates at low temperature (~ 200 °C) [10]. It was found that AlN resonator exhibits photo-sensitive property in addition to thermal effects when exposed to IR source.

DESIGN AND FABRICATION

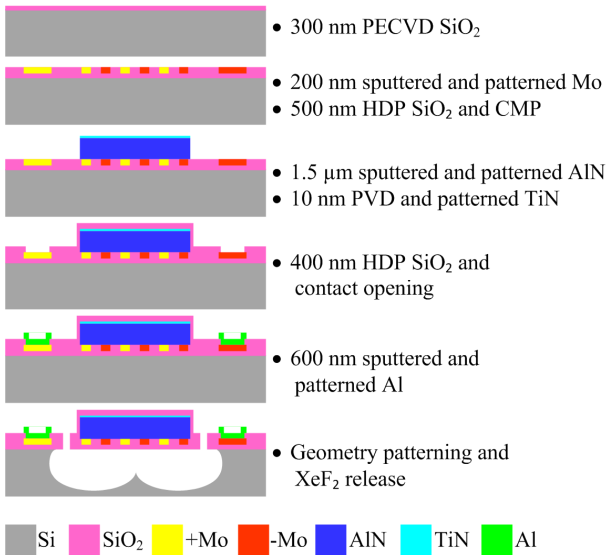

Figure 1: The schematic process flow of the AlN resonant IR detector.

Figure 1 shows the schematic process flow of the AlN resonant IR detector. The device was fabricated on top of a PECVD SiO_2 support layer (300nm thick). After the sputtering and patterning of Mo bottom excitation electrodes

(200 nm thick with 2 µm pitch), a HDP SiO_2 layer (500 nm thick) was deposited and flatten until Mo electrodes by CMP. AlN piezoelectric thin film (1.25 µm thick) and TiN-absorber (10 nm thick) was then deposited by sputtering and patterned to define the IR detector pixel geometry (48 µm x 48 µm). The 10 nm TiN is designed to enhance the IR absorption by matching the atmospheric impedance (377 Ω/□) and also to act as floating electrode for the AlN resonator. Since the TiN layer is extremely thin, there is no tradeoff issue between absorptivity and *Q*-factor caused by the mechanical mass loading effect. Another layer of HDP SiO_2 (400 nm) was deposited to passivate the device, followed by Al contact pads (600 nm thick) formation and release hole opening. The device was finally released by XeF_2 to have a freestanding AlN resonator as illustrated by the SEM image in Figure 2.

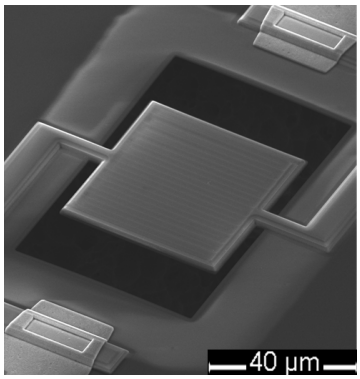

Figure 2: The SEM image of the fabricated AlN resonant IR detector.

RESULTS AND DISCUSSION

The experiment setup in this work is shown in Figure 3. The device under test (DUT) was placed on a temperature chuck inside a vacuum chamber. Before the frequency response measurements of the fabricated device were taken, a Short-Open-Load-Thru (SOLT) impedance calibration of the GSG probes and network analyzer (Agilent E5071B) was carried out to ensure the results accuracy. The measured and modified-Butterworth van Dyke (MBVD) fitted admittance-frequency curves of the AlN resonator is plotted in Figure 4. The device has a resonant frequency of 2.336 GHz and *Q*-factor of ~ 830.

A blackbody source (BS) from ORIEL Instruments with different temperatures was used to emit a spectrum of IR radiation. An optical filter with transmitted wavelength of 0.5 µm to 20 µm was used to isolate ultraviolet (UV) light. To further eliminate visible light, a 725 µm thick Si wafer was placed above the optical filter. Figure 5 illustrates the change in S_{21} magnitude at resonant frequency with different BS temperatures. A smaller shift of S_{21} magnitude was observed with additional Si wafer filter which proves that the device is responsive to IR wavelength longer than 1.12 µm.

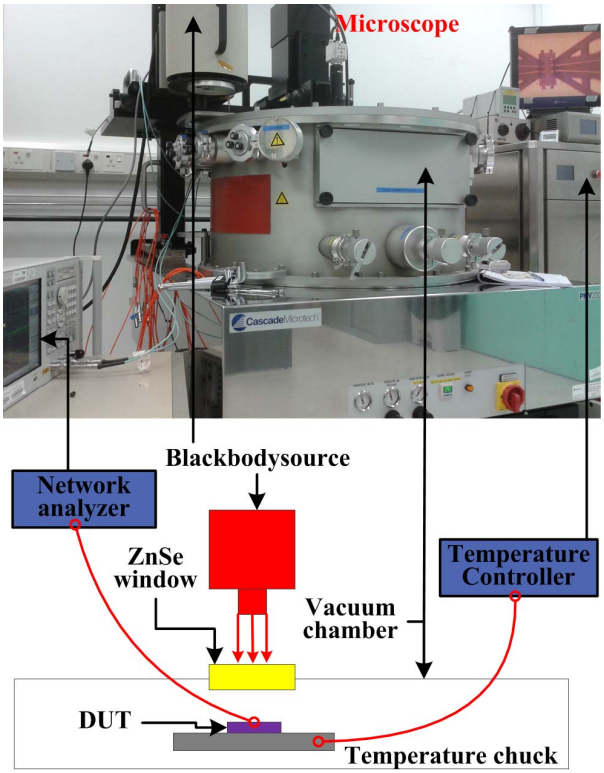

Figure 3: The experiment setup for frequency response measurement of the AlN resonant IR detector.

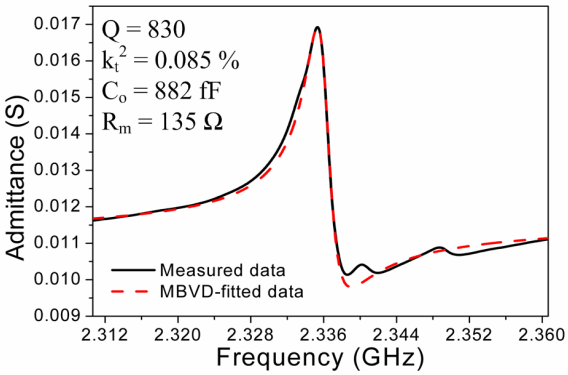

Figure 4: The measured and MVVD-fitted admittance of the AlN resonant IR detector.

It is worth noting that there is no significant shift in resonant frequency under different BS temperatures as observed from Figure 5. This observation is different from other works which reported on the shift of resonant frequency resulted from thermal effect [7-9]. To further investigate this phenomenon, the frequency response of the device was measured at different chuck temperatures and the effective temperature coefficient of frequency (TCF) was extracted as depicted in Figure 6. Due to the comparable thickness of SiO_2 with AlN, the positive TCF of SiO_2 dominates in the device effective TCF [11] which has a value of +19.69 ppm/K.

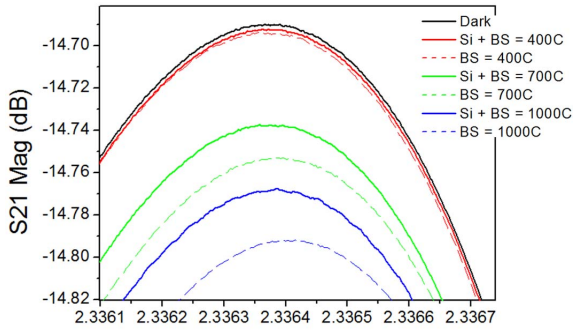

Figure 5: The measured S_{21} magnitude of the AlN resonant IR detector under different BS temperatures. (Si = Si wafer filter)

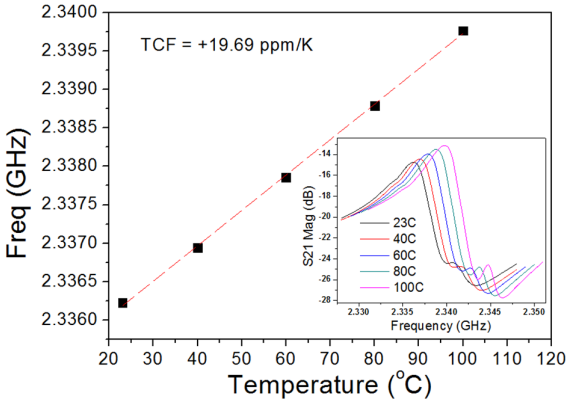

Figure 6: The temperature dependent resonant frequency of the AlN resonant IR detector.

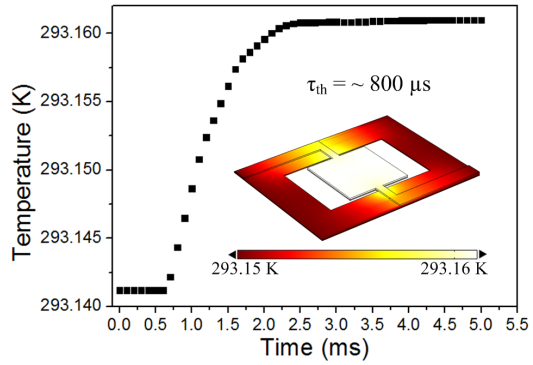

Figure 7: The simulated temperature profile and the thermal time constant of the AlN resonant detector at P_{IR} of 615 nW. .

COMSOL Multiphysics tool was employed to estimate the temperature profile of the device as shown in Figure 7. The material properties of AlN, SiO_2 and Mo used in this transient time simulation are summarized in Table 1. An IR power, P_{IR} of 615 nW (BS temperature of 1000 °C) rises the device temperature by less than 0.02 K which translated to a 920 Hz of upshift in resonant frequency assuming a full absorption. Detecting this small amount change of resonant frequency in a GHz-device is a great challenge due to temperature fluctuation, power supply noise and the network analyzer resolution limit.

Table 1: Material properties of AlN, SiO_2 and Mo used in the thermal simulation.

Material properties	AlN	SiO2	Mo
Thermal conductivity [W/ (m·K)]	185	1.4	138
Mass density [kg/m^3]	3260	2200	10200
Heat capacity [J/(kg·K)]	740	730	250

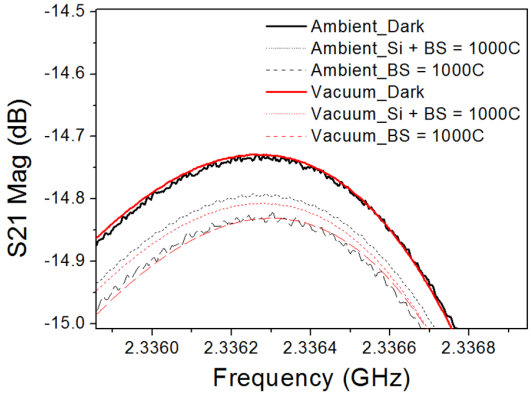

Figure 8: Comparison of IR sensing performance of the AlN resonant IR detector under ambient (black color curves) and vacuum (red color curves) condition.

The IR sensing performance of the device was then compared under ambient and vacuum conditions. The ambient measurement data is noisier due to the scratch of the device contact pads as it was done after the vacuum measurement. Figure 8 shows no significant difference in S_{21} magnitude shift between the ambient and vacuum measurement results. This observation strongly proves that there is no thermal effect involved in the IR responsivity. The reasons of the shift of S_{21} magnitude in response to the IR exposure is still unclear and has not been studied before. Similar observation has been reported in [12] for the wavelength range of visible light. It was explained that the defect-induced sub-bandgap absorptions is the main contribution of the photoresponse. However, it is believed that there are other mechanisms that could cause the IR sensitivity of AlN in this work including impurities-related energy states transitions [13] or polarization distortion caused by phonon absorption [14, 15], where both the occurrences can also alter the static capacitance of AlN and thus the admittance of the frequency response . In any event, a more in depth study and characterization are needed to explain this phenomenon.

At P_{IR} of 615 nW, a -0.102 dB shift of S_{21} magnitude was obtained corresponding to a IR responsivity, $\Re$ of 166 kdB/W. The root mean squared (RMS) noise, V_n of the measured S_{21} magnitude in 1 Hz bandwidth was obtained to be 56.9 µdB/√Hz. The device IR detectivity, D^* of 1.41 × 10^7 cm√Hz/W was calculated using the equation below.

$$D^* = \frac{\Re \cdot \sqrt{A_B}}{V_n} \quad (1)$$

where A_B is the pixel area of the AlN resonant IR detector.

CONCLUSION

This paper demonstrates the capability of AlN-based IR detector to operate without the need of vacuum and cooling system. This brings the great advantage in device packaging and thus further reduces the manufacturing and operation cost compared with thermal detectors and photon detectors. Even though the estimated detectivity of the current design is about two orders of magnitude lower than the commercial resistive bolometers, it is believed that the performance can be boosted up by either device structure optimization or IR absorptivity enhancement. Thus, the detailed physics and mechanisms have to be first understood before the optimization steps.

ACKNOWLEDGEMENTS

The authors are grateful to the clean room staffs in Institute of Microelectronics, A*STAR, Singapore for their supports in fabrication process. GLOBALFOUNDRIES Singapore Pte Ltd and Singapore Economic Development Board are acknowledged for the scholarship of the PhD program offered to one of the authors at Nanyang Technological University (NTU). Funding is provided by A*STAR, Singapore (#1021650084). C.S. Tan is grateful for the support from the Silicon Technologies Center of Excellence (Si-COE) and Nanoelectronics Centre of Excellence (NOVITAS) at NTU.

REFERENCES

[1] X. Shao, J. Ding, X. Ma, Y. Yu, and J. Fang, "Design and thermal analysis of electrically calibrated pyroelectric detector," *Infrared Physics & Technology,* vol. 55, pp. 45-48, 2012.

[2] X. Dehui, X. Bin, W. Guoqiang, M. Yinglei, and W. Yuelin, "Uncooled Thermoelectric Infrared Sensor With Advanced Micromachining," *IEEE Sensors Journal,* vol. 12, pp. 2014-23, 2012.

[3] A. Tazzoli, M. Rinaldi, and G. Piazza, "Experimental Investigation of Thermally Induced Nonlinearities in Aluminum Nitride Contour-Mode MEMS Resonators," *IEEE Electron Device Letters,* vol. 33, pp. 724-6, 2012.

[4] J. E. Ralph, R. C. King, J. E. Curran, and J. S. Page, "Miniature quartz resonator thermal detector," in *IEEE 1985 Ultrasonics Symposium. Proceedings. (Cat. No.85CH2209-5), 16-18 Oct. 1985*, New York, NY, USA, 1985, pp. 362-4.

[5] M. R. Hamrour and S. Galliou, "Analysis of the infrared sensitivity of a quartz resonator application as a thermal sensor," in *Proceedings of IEEE Ultrasonics Symposium, 1-4 Nov. 1994*, New York, NY, USA, 1994, pp. 513-16.

[6] M. B. Pisani, K. Ren, P. Kao, and S. Tadigadapa, "Application of Micromachined y -cut-quartz bulk acoustic wave resonator for infrared sensing," *Journal of Microelectromechanical Systems,* vol. 20, pp. 288-296, 2011.

[7] M. Rais-Zadeh, "Gallium nitride micromechanical resonators for IR detection," in *Micro- and Nanotechnology Sensors, Systems, and Applications IV, 23-27 April 2012*, USA, 2012, p. 83731M (6 pp.).

[8] Z. Wang, X. Qiu, S. J. Chen, W. Pang, H. Zhang, J. Shi, and H. Yu, "ZnO based film bulk acoustic resonator as infrared sensor," *Thin Solid Films,* vol. 519, pp. 6144-6147, 2011.

[9] Y. Hui and M. Rinaldi, "High performance NEMS resonant infrared detector based on an aluminum nitride nano-plate resonator," in *2013 Transducers & Eurosensors XXVII: 17th International Conference on Solid-State Sensors, Actuators and Microsystems (TRANSDUCERS & EUROSENSORS XXVII), 16-20 June 2013*, Piscataway, NJ, USA, 2013, pp. 968-71.

[10] A. Fardeheb-Mammeri, M. B. Assouar, O. Elmazria, J. J. Fundenberger, and B. Benyoucef, "Growth and characterization of c-axis inclined AlN films for shear wave devices," *Semiconductor Science and Technology,* vol. 23, p. 095013 (7 pp.), 2008.

[11] J. H. Kuypers, C.-M. Lin, G. Vigevani, and A. P. Pisano, "Intrinsic temperature compensation of aluminum nitride Lamb wave resonators for multiple-frequency references," in *2008 IEEE International Frequency Control Symposium, FCS, May 19, 2008 - May 21, 2008*, Honolulu, HI, United states, 2008, pp. 240-249.

[12] C. J. Zhou, Y. Yang, Y. Shu, H. L. Cai, T. L. Ren, M. Chan, J. Zhou, H. Jin, S. R. Dong, and C. Y. Yang, "Visible-light photoresponse of AlN-based film bulk acoustic wave resonator," *Applied Physics Letters,* vol. 102, p. 191914 (3 pp.), 2013.

[13] H. M. Huang, R. S. Chen, H. Y. Chen, T. W. Liu, C. C. Kuo, C. P. Chen, H. C. Hsu, L. C. Chen, K. H. Chen, and Y. J. Yang, "Photoconductivity in single AlN nanowires by subband gap excitation," *Applied Physics Letters,* vol. 96, p. 062104 (3 pp.), 2010.

[14] M. Kazan, B. Rufflé, C. Zgheib, and P. Masri, "Phonon dynamics in AlN lattice contaminated by oxygen," *Diamond and Related Materials,* vol. 15, pp. 1525-1534, 2006.

[15] C. Balasubramanian, S. Bellucci, G. Cinque, A. Marcelli, M. C. Guidi, M. Piccinini, A. Popov, A. Soldatov, and P. Onorato, "Characterization of aluminium nitride nanostructures by XANES and FTIR spectroscopies with synchrotron radiation," *Journal of Physics: Condensed Matter,* vol. 18, pp. 2095-104, 2006.

CONTACT

*W. C. Ang, Tel: +65-81235074; wcang1@e.ntu.edu.sg